Available online at BCREC Website: http://bcrec.undip.ac.id

Bulletin of Chemical Reaction Engineering & Catalysis, 12 (3), 2017, 469-477

Research Article

Synthesis and Performance of Transition Metal Based Perovskite Catalysts for Diesel Soot Oxidation

Anupama Mishra[1,2*], R. Prasad[2]

[1]Department of Chemical Engineering, University of Petroleum and Energy Studies, Dehradun-248007, Uttarakhand, India
[2]Department of Chemical Engineering and Technology, Indian Institute of Technology (Banaras Hindu University), Varanasi 221005, Uttar Pradesh, India

Received: 2nd March 2017; Revised: 16th June 2017; Accepted: 12nd July 2017; Available online: 27th October 2017; Published regularly: December 2017

Abstract

In present investigation, the effect of the intrinsic factors including the structure, nature of B-site ions in the four systems $LaCoO_3$, $LaNiO_3$, $LaFeO_3$ and $LaZnO_y$ perovskite-type oxide catalysts, and the external factors of catalyst-soot contacting model, and the operating parameters such as air flow rate and temperature on the catalytic performances for the combustion of diesel soot were reported. The catalysts were characterized by XRD, FTIR, SEM, and N_2-sorption. Activity of the catalyst for soot oxidation was evaluated on the basis of light off temperature characteristics T_i, T_{50} and T_{100}. $LaCoO_3$, $LaFeO_3$ and $LaNiO_3$ samples possessed the perovskite structure, and gave high activities for the total oxidation of soot below 445 °C. Whereas, $LaZnO_y$ catalyst was not indicating the ABO_3 perovskite structure and existed as a mixture of metal oxides. The activity order in decreasing sequence of the catalyst was as follows: $LaCoO_3$>$LaFeO_3$>$LaNiO_3$>$LaZnO_y$. SEM pictures of the perovskite samples showed that the particles sizes were close to 100 nm.

Keywords: Perovskite; Soot oxidation; Soot-catalyst contact; Air flow rate

How to Cite: Mishra, A., Prasad, R. (2017). Synthesis and Performance of Transition Metal Based Perovskite Catalysts for Diesel Soot Oxidation. *Bulletin of Chemical Reaction Engineering & Catalysis*, 12 (3): 469-477 (doi:10.9767/bcrec.12.3.968.469-477)

Permalink/DOI: https://doi.org/10.9767/bcrec.12.3.968.469-477

1. Introduction

Diesel engines have a variety of advantages over other engines types, such as higher fuel economy, reliability, durability as well as lower fuel and maintenance costs. Diesel engines have a variety of advantages over other engines types, such as higher fuel economy, reliability, durability as well as low maintenance costs [1]. Despite these advantages diesel engines have some drawbacks, one of which is high amount of particulate matter (PM) emissions, which mainly consist of carbonaceous soot and soluble organic fraction (SOF) of hydrocarbons [2]. The majorities of the components emitted from diesel exhaust are mutagens, carcinogens and toxic air pollutants and is suspected in a series of adverse effects [3]. Particularly the soot particle causes health problems, pollution of air, water, and soil, soiling of buildings, reductions in visibility, impact agriculture productivity, global climate change, etc.

Catalyst coated diesel particulate filter (DPF) is an efficient device to trap and burn the diesel PM. Many types of catalysts for the DPF

* Corresponding Author.
E-mail: amishra@ddn.upes.ac.in (Mishra, A.)
Telp.: +918171257955

have been investigated for the soot combustion; platinum group metals (PGM), Perovskite-type oxides, spinel type oxides and mixed transition metal oxides [4]. Most of perovskite-type oxides, meet the requirements for soot oxidation, and thus many kinds of bulk perovskite-type oxides have been prepared and studied in order to improve the performances for soot oxidation. The redox property of a perovskite-type oxide is closely related to the nature of B-site or A-site cations. Some researchers [5-8] have proved that the perovskite-type oxide catalysts exhibit much better catalytic performances for the title reaction than that of simple oxide.

There is no study reported on the effect of different B-site ions in ABO_3 perovskite structure for the catalytic oxidation of diesel soot. Further, no report is available in the literature regarding the optimization of various operating parameters for diesel soot oxidation. Thus, in this article, the physico-chemical properties and catalytic performances of Ni-, Co-, Fe-, and Zn- based perovskite-type complex oxide catalysts for the removal of diesel soot were comparatively and systematically studied. The effects of the intrinsic factors including nature of B-site ions, redox properties of perovskite-type composite oxide catalysts, and the external factors containing contact model of catalyst and soot, and the air flow rate on their catalytic performances for the elimination of soot particles were also investigated.

2. Experimental

2.1 Preparation of soot

The soot was prepared by partial combustion of locally available commercial diesel (HP) in lamp with limited supply of air, and collected on the inner walls of an inverted beaker. The soot was collected from the recipient walls and then dried in an electric oven for overnight at 120 ^oC.

2.2 Preparation of catalysts

A series of perovskite-type oxide catalysts were prepared by the sol-gel method. All AR-grade chemicals were used in the preparation of catalysts. Three different set of La based perovskite, $LaCoO_3$, $LaFeO_3$ and $LaNiO_3$, were prepared by citric acid sol-gel method. For the preparation of $LaCoO_3$ aqueous solution (0.1M) of $La(NO_3)_3.6H_2O$ and $Co(NO_3)_2.6H_2O$ were mixed with citric acid that was equivalent in gram mole with that of the total cations (La^{3+} and Co^{2+}). Resulting red wine colored solution was heated at 80 ^oC under continuous stirring. After 3 h of continuous stirring the clear solution gradually transformed into gel which was translucent and viscous. The wet gel was dried homogeneously overnight in oven at 120 ^oC in presence of air. Obtained loose and foamy pink color solid was heated in two steps. First heating at 600 ^oC for 1 h is carried out to decompose the organic and second step of calcination was done at 750 ^oC for 4 h to obtain hazy black porous solid. $LaFeO_3$ and $LaNiO_3$ perovskite were prepared in the similar fashion from their nitrate precursors $Fe(NO_3)_3.9H_2O$ and $Ni(NO_3)_2.6H_2O$, respectively.

A mixed metal oxide $LaZnO_y$ with same stoichiometric composition as required for perovskite formation $LaZnO_3$ was also prepared by the citric acid sol-gel method. Aqueous solution (0.1 M) of $La(NO_3)_3.6H_2O$ and $Zn(NO_3)_2.6H_2O$ were mixed with citric acid that was equivalent in gram mole with that of the total cations (La^{3+} and Zn^{2+}). Resulting colorless solution was heated at 80 ^oC under continuous stirring. After 3 h of continuous stirring the clear solution gradually transformed into gel which was translucent and viscous. The wet gel was dried homogeneously overnight in oven at 120 ^oC in presence of air. Obtained off-white colored loose and foamy solid was heated at 600 ^oC for 1 h and further grained before calcining it at 750 ^oC for 4 h and finally obtained white colored porous solid.

2.3 Catalyst testing

The catalytic performances of the prepared catalysts for oxidation of soot were evaluated in a compact fixed bed tubular quartz reactor shown as inset in Figure 1. The reactor was consisting of two co-axial glass tubes of 20 mm and 50 mm diameter. A helical coil of quartz tube in between the co-axial tubes served as a pre-heater of the air. There is a hole in the lower part of the outer tube, to take care of breakage due to the expansion or contraction of air in between co-axial tubes as the unit is subjected to the variation of temperature from ambient to the reaction temperature. The pre-heated air enters the catalyst bed, kept in the inner tube as shown in the figure. The product stream from the bottom of the reactor is cooled in a condenser to the ambient temperature and then analyzed with the help of an online Gas chromatograph.

The reactor was mounted vertically in a split open furnace. The down flow stream of air was used to avoid the distortion of the bed. The soot-catalyst (catalyst bed diameter 20 mm and height 1.27 mm) was placed on a thin layer of

glass wool which is supported on perforated quartz disc inside the inner tube. A thermocouple well made of 4 mm diameter tube was inserted axially from the bottom all the way to the centre of the disc for temperature measurement and control. The catalytic activity was evaluated by placing 110 mg catalyst-soot mixture in the reactor, and the oxidation was carried out in the temperature range from ambient to total conversion of soot at a constant heating rate of 1 ^{o}C min^{-1}. Before the reaction, the soot-catalyst mixture, in a 1/10 weight ratio, were milled in an agate mortar for "tight contact" and with spatula for loose contact. The inlet air was fed to the reactor with a steady flow rate of 150 mL min^{-1}. To verify the reproducibility of the experimental data each experiment was performed twice repeatedly for the soot oxidation.

2.4 Calculation of the soot conversion

A graph between chromatogram areas for CO_2 vs. increasing temperature for catalytic soot oxidation was plotted as shown in Figure 2 for a typical experimental run. The fractional conversion of soot, (X) is defined as:

$$X = (M_o\text{-}M)/M_o \quad (1)$$

where, M_o is the weight of initial soot taken, which is proportional to total area of the graph bounded between temperature of initiation of soot oxidation (T_o) and temperature for 100 % oxidation of soot (T_{100}), can be given as (equation 2).

$$Mo\alpha \sum_{To}^{T_{100}} A_{CO_2}\Delta T \quad (2)$$

where M is the weight of soot at a typical temperature (T_i), higher than the temperature (T_o). The weight loss (M_o-M) at temperature T_i, which is proportional to the area bounded by the graph between T_o and T_i, can be given as equation 3.

$$(Mo-M)\alpha \sum_{To}^{T_i} A_{CO_2}\Delta T \quad (3)$$

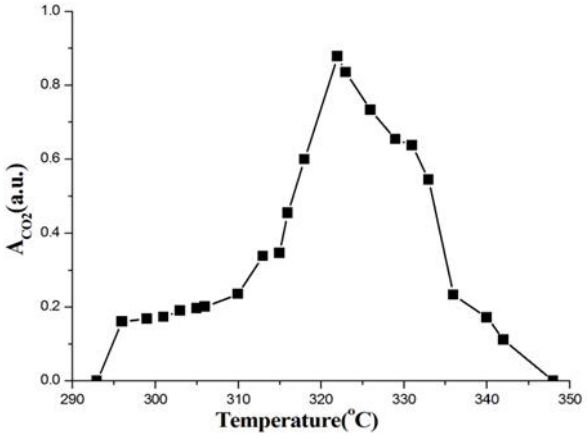

Figure 2. A typical graph between chromatogram areas for CO_2 vs. temperature

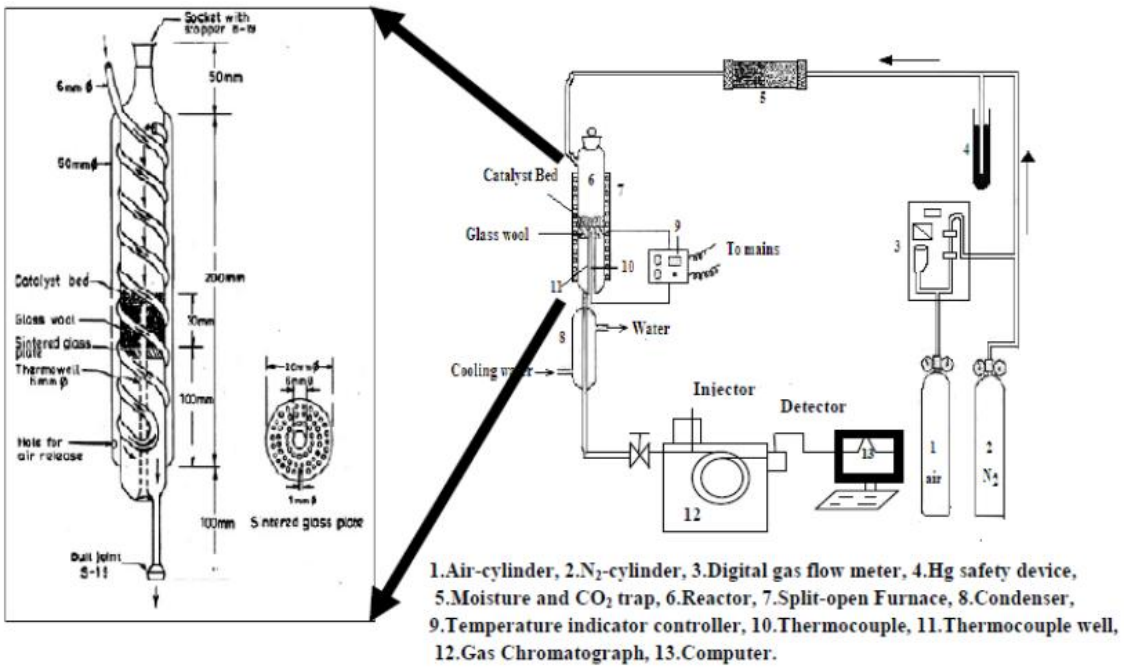

Figure 1. Schematic diagram of experimental setup

Therefore, the value of X at various extent of reaction can be calculated using the following formula (equation 4):

$$X = \frac{\sum_{To}^{Ti} A_{CO_2} \Delta T}{\sum_{To}^{T_{100}} A_{CO_2} \Delta T} \quad (4)$$

2.5 Catalyst characterization

The textural characterization of the catalysts was carried out by low temperature N_2-sorption method using a Micromeritics ASAP 2020 analyzer. Phase identification of the catalysts were carried out by X-ray diffraction (XRD) patterns on a powder X-ray diffractometer (Rigaku Ultima IV) using CuKα (λ = 1.5405 Å) radiation with a nickel filter operating at 40 mA and 40 kV. FTIR spectra of the catalysts were recorded in the range of 400-4000 cm^{-1} on Shimadzu 8400 FTIR spectrometer with KBr pellets at room temperature. XPS of the catalysts was performed on an Amicus spectrometer equipped with MgKα X-ray radiation. For typical analysis, the source was operated at a voltage of 15 kV and current of 12 mA. Pressure in the analysis chamber was less than 10^{-5} Pa. The binding energy scale was calibrated by setting the main C 1s line of adventitious impurities at 284.7 eV, giving an uncertainty in peak positions of ±0.2 eV.

3. Results and Discussion

3.1 Textural characterization of the catalysts

The textural properties including BET surface area, total pore volume and average pore diameter of the perovskites studied in the present investigation are summarized in Table 1. It can be seen from the table that the various perovskite have low specific surface area (4-9 m^2/g) and average pore diameter (36-42 Å), which is in expected range considering the high synthesis temperature in accordance with references [9,10]. The $LaCoO_3$ sample, calcined at 750 °C in stagnant air, showed the highest surface area (09.12 m^2/g). Similarly, the catalyst of $LaNiO_3$ and calcined in air, displayed the lowest surface area (4.80 m^2/g). It is very interesting to note that the catalyst of $LaZnO_y$ exhibited the lowest pore diameter (36.67 Å) and comparable average pore volume (0.0087 cm^3/g) as compared to other catalysts prepared.

3.2 XRD characterization of the catalysts

The powder XRD patterns of catalyst samples prepared by citric acid sol-gel method are shown in Figure 3. The XRD peaks were found to be very sharp indicating that the ABO_3 perovskite structure is well maintained in $LaCoO_3$ (A), $LaFeO_3$ (B), and $LaNiO_3$ (C). Instead of expectation in the catalyst of $LaZnO_y$ perovskite structure is totally inaccessible. In Figure 3, the obtained XRD data were compared with the standard JCPDS pattern for $LaCoO_3$ (with JCPDS card No. 25-1060), $LaFeO_3$ (with JCPDS card no. 37-1493) and $LaNiO_3$ (with JCPDS card no.33-0711) while in $LaZnO_y$ shows the presence of La_2O_3 (with JCPDS card No. 83-1344), $La(OH)_3$ (with JCPDS card No. 83-2034), and ZnO (with JCPDS card No. 89-1397) as the main crystal-

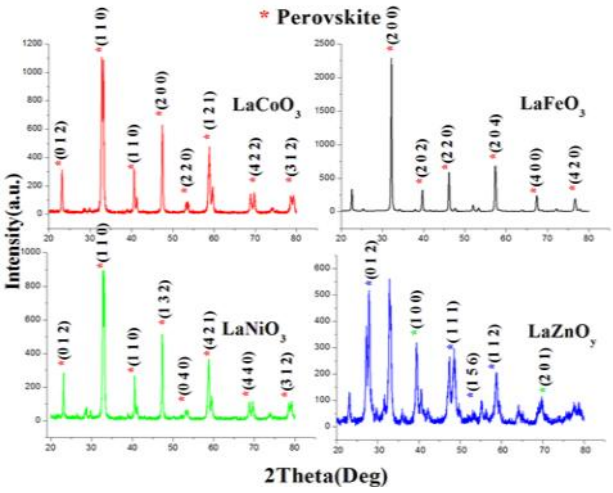

Figure 3. XRD Pattern of (A) $LaCoO_3$, (B) $LaFeO_3$, (C) $LaNiO_3$ and (D) $LaZnO_y$

Table 1. Textural characterization of perovskite catalyst samples

Catalyst	BET surface area (m^2/g)	Pore volume (cm^3/g)	Average pore diameter (Å)
$LaCoO_3$	09.12	0.0074	41.70
$LaFeO_3$	07.91	0.0081	40.23
$LaNiO_3$	04.80	0.0096	42.89
$LaZnO_y$	05.87	0.0087	36.67

line phase. The crystallite size was estimated using the Scherrer equation (5) which is given by Equation 5.

$$d = 0.89\lambda/\beta \cos\theta \quad (5)$$

where d, λ, θ, and β are the crystallite size, X-ray wavelength (1.518 Å), Bragg diffraction angle and full width of the half maximum (FWHM) of the diffraction peak, respectively, and the crystallite size data are reported in Table 2. The crystallite size values were found in the range of 14.52-33.50 nm. $LaNiO_3$ shows the smallest crystallite size of 14.52 nm, whereas the $LaCoO_3$ shows the largest crystallite size of 32.13 nm.

In the catalyst of $LaZnO_y$ the presence of $La(OH)_3$ phase is very unusual as calcination of sol-gel precursors at 750 °C decomposes lanthanum compounds purely into La_2O_3 according to following reactions (Equations 6 and 7) [11].

$$La(OH)_3 \xrightarrow{300-400^oC} LaOOH \xrightarrow{400-500^oC} La_2O_3 \quad (6)$$

$$La_2O_2CO_3 \xrightarrow{400-460^o} La_2(CO_3)_3 \xrightarrow{460-550^oC} La_2O_2CO_3 \xrightarrow{>600^oC} La_2O_3 \quad (7)$$

However, the presence of $La(OH)_3$ in the XRD diffractogram (Figure 3(D)), indicates that exposure of catalysts to ambient conditions favors hydroxylation of La_2O_3.

3.3 FTIR characterization of the catalysts

The FTIR spectra in the range 4000-400 cm^{-1} of the catalysts prepared are shown in Figures 4 and 5. Figure 4 depicts the FTIR spectra of the perovskite catalysts ($LaCoO_3$, $LaFeO_3$ and $LaNiO_3$) calcined at the 750 °C in stagnant air. The broad absorption bands around 3054 cm^{-1} and 2306.2 cm^{-1} appeared in the IR spectra corresponded to OH stretching and OH bending of water. The absorption band at 1408 cm^{-1} was corresponded to nitrate ion. In addition, the band at 1096 cm^{-1} was corresponded to Co–OH bending which is confirmed with the reported value that MOH bending mode appears below 1200 cm^{-1} [12]. The absorption band at ~600 cm^{-1} are ascribed to Co-O/Fe-O/Ni-O and MO_6 stretch vibrations in the perovskite structure.

Figure 5 shows the FTIR spectra of $LaZnO_y$. An intense and sharp band at 3609.4 cm^{-1} is assigned to the stretching and bending O–H vibrations of lanthanum hydroxide [13]. Bands near 3444 cm^{-1} represent the O–H stretching

Table 2. The crystallite size of all the catalysts

Catalyst	Crystallite size (nm)		
$LaCoO_3$	32.13		
$LaFeO_3$	25.12		
$LaNiO_3$	14.52		
$LaZnO_y$	La_2O_3	$La(OH)_3$	ZnO
	33.5	23	27.1

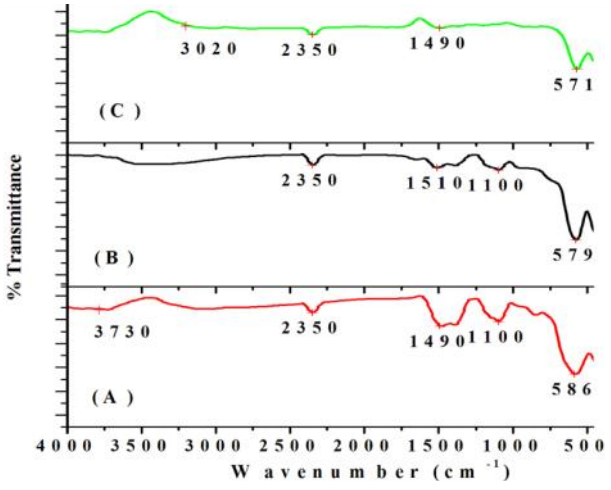

Figure 4. FTIR spectra of (A) $LaCoO_3$, (B) $LaFeO_3$, (C) $LaNiO_3$

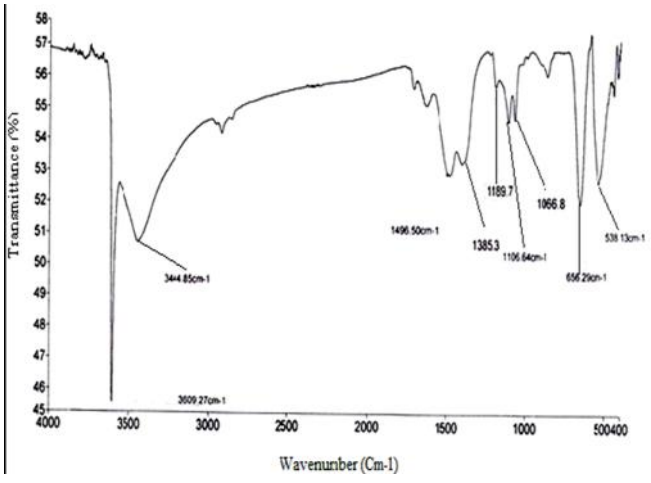

Figure 5. FTIR spectra of the $LaZnO_y$

mode indicative of the presence of adsorbed water on the sample surface [14] and peaks at 1496 and 1385 cm^{-1} shows $La_2O_2CO_3$ [15]. The strong peak at 1066 cm^{-1} is assigned to the Zn–O–H bending. The peaks of 538.13 cm^{-1} and 656.29 cm^{-1} shows the characteristics peak of ZnO and La_2O_3 [16].

3.4 SEM characterization of the catalysts

The SEM images of LaZnOy at different magnifications shown in Figure 6 revealed that the prepared catalyst sample was highly porous, less aggregated and surface of the catalyst appears to be spongy tendrils. The particle size of the mixed oxides is small and uniformly distributed. The SEM images (Figure 6) clearly show the difference in surface morphology due to presence of different B-site ions (Co, Fe, and Ni). In comparison to $LaCoO_3$ other two perovskite ($LaFeO_3$ and $LaNiO_3$) were more aggregated and porus surface can be visualized (Figure 7F and G). Morphological microscopy of the explored samples also demonstrated agglomerates involved mostly thin, smooth flakes and layers perforated by a large number of pores.

3.5 Catalysts activity test

The catalytic combustion tests were performed with a flow rate 150 mL//min over the catalyst samples prepared by sol-gel method as a function of temperature. The reproducibility of the experimental data was confirmed by repeating some of the tests for a few times, as illustrated in Figure 8. A long-term activity test was also carried out, after reaching the tem-

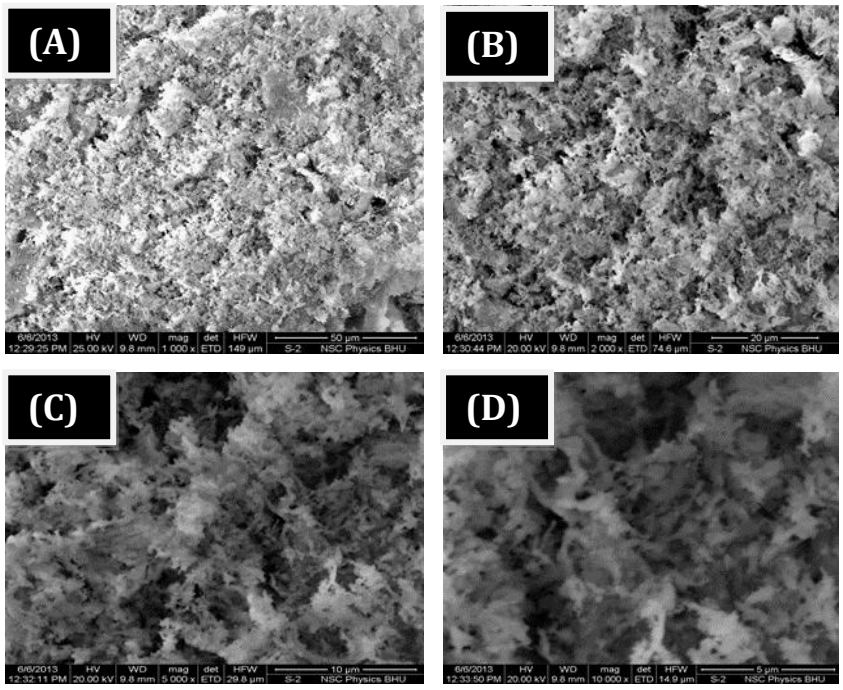

Figure 6. SEM images of $LaZnO_y$ catalyst; (A) 1000x (B) 2,000x (C) 5,000xs, and (D) 10,000x magnification

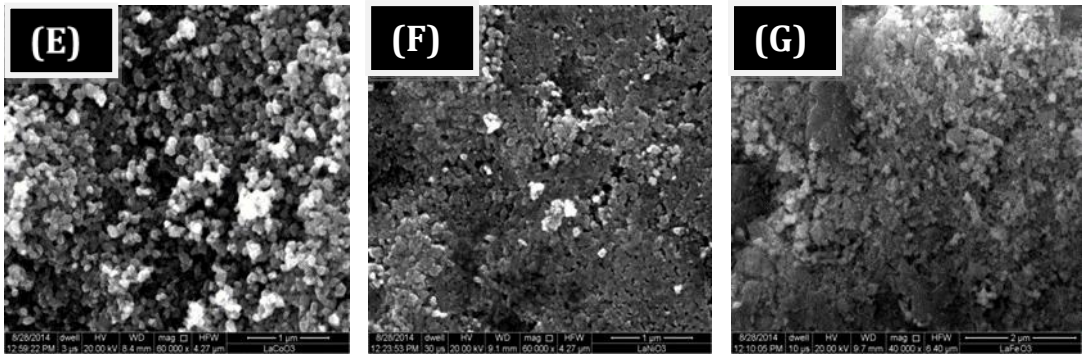

Figure 7. SEM images of (E) $LaCoO_3$,(F) $LaFeO_3$, (G) $LaNiO_3$

perature of T_{100} (100 % soot combustion). The reaction was then continued at the constant temperature of T_{100} for at least 7 h. No change in the catalyst activity was ever observed. Activity of the catalyst for soot oxidation was evaluated on the basis of light off temperature characteristics T_i, T_{50}, and T_{100} where, T_i, T_{50}, and T_{100} are temperature corresponding to the start of soot ignition, the 50 % conversion of soot and total oxidation of soot respectively. Experiments for the soot oxidation were planned to run up-to maximum temperature of 450 °C which can be achieved by the diesel exhaust. Experiments were conducted to see the effect of transition metal Ni, Co, Fe, and Zn at the B-site of the ABO_3 perovskite on soot oxidation represented in Figure 8 and also in Table 3. Four catalysts $LaCoO_3$, $LaNiO_3$, $LaFeO_3$, and $LaZnO_y$ were tested for soot oxidation. Figure 8 shows that the combustion of diesel soot started at light off temperature (T_i) 290, 319, 336, and 376 °C for the catalysts of $LaNiO_3$, $LaFeO_3$, $LaCoO_3$, and $LaZnO_y$, respectively. The catalytic activity of the perovskite samples chiefly depends on three factors: chemical composition, degree of crystallinity, and the crystals morphology (including particle sizes, pore size distribution, and specific surface area of the perovskite catalyst). All these factors are affected by the synthesis method and the specific synthesis operating conditions.

Experiments were also conducted to study the effect of air flow rate on soot oxidation over $LaCoO_3$ for soot oxidation at four different flow rates (50 mL/min, 100 mL/min, 150 mL/min, and 200 mL/min). Figure 9 shows that increasing flow rate from 50 to 150 mL/min cause decrease in the characteristic temperatures (T_i, T_{50}, T_{100}) while further increase in flow rate cause increase in characteristic temperatures. This phenomenon explains two counter effects of increasing flow rate on soot oxidation. Increasing flow rate of air leads to more oxidants (O_2), which helps to improve the combustion of soot particle. On the other hand increase in the air flow rate shortens the resident time of the reactants which negatively affect the soot oxidation. These two counter affects gives optimum value of air flow rate at 150 mL/min having lowest characteristic temperatures (T_i=336 °C, T_{50}=389 °C, and T_{100}=420 °C).

Table 4 shows characteristic temperatures of soot oxidation at different flow rates. A loose contact study was also carried out to simulate the actual circumstances of diesel particulate filter [17]. Figure 10 shows a comparison of conversion of soot particles over $LaCoO_3$ under tight and loose contact conditions of the catalyst-soot. It can be visualized from Figure 8 that lower activity under loose contact than under tight contact existed. The observation is obvious as the catalysis is a surface phenomenon,

Table 3. Light off temperatures of perovskite-type catalysts

Catalysts	T_i (°C)	T_{50} (°C)	T_{100} (°C)
$LaCoO_3$	336	389	420
$LaFeO_3$	319	397	428
$LaNiO_3$	290	392	441
$LaZnO_y$	376	426	456

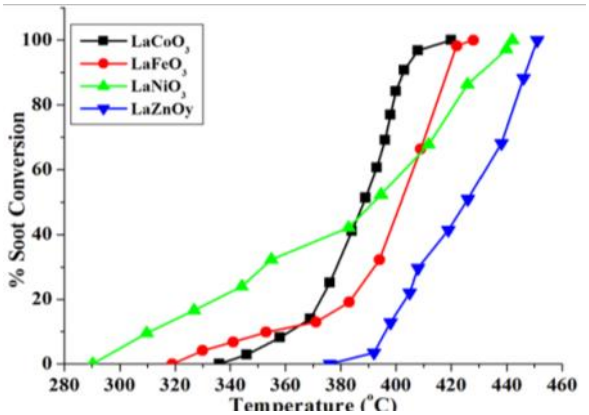

Figure 8. Soot conversion over Perovskite-type Catalysts, Calcined at 750 °C, Catalyst/ Soot: 10/1, Tight Contact, Air flow rate: 150 mLmin

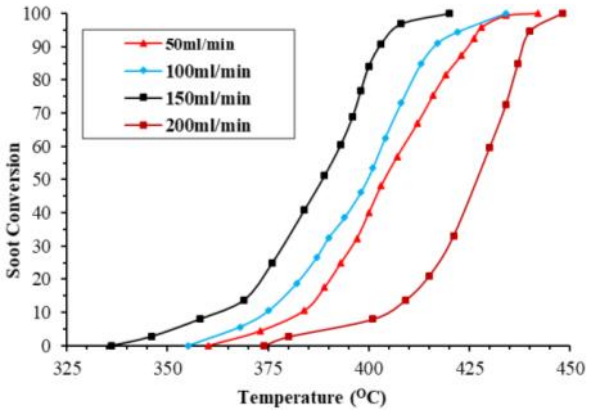

Figure 9. Effect of air flow rate on soot oxidation over $LaCoO_3$

Table 4. Effect of air flow rate on soot oxidation over $LaCoO_3$

Flow rate (mL/min)	T_i (°C)	T_{50} (°C)	T_{100} (°C)
50	360	404	442
100	355	400	434
150	336	389	420
200	374	425	448

Table 5. Effect of contact type on soot oxidation on $LaCoO_3$ catalyst

Contact condition	T_i	T_{50}	T_{100}
Tight contact	336	389	420
Loose contact	376	438	472

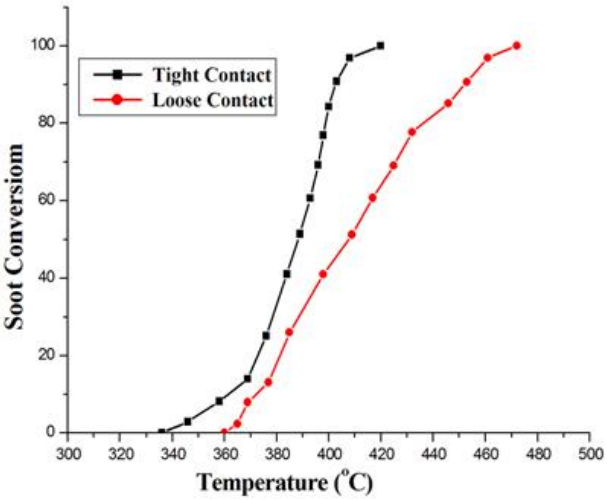

Figure 10. Effect of contact type on soot oxidation on $LaCoO_3$ catalyst, calcination 750 °C catalyst/soot: 10/1, air flow rate: 150 mL/min

higher the surface contacts (tight contact) higher the activity. From the Table 5, it is clear that the $LaCoO_3$ resulted complete soot oxidation at T_{100} = 472 °C under loose contact which is 52 °C higher than tight contact. The catalytic activity for soot oxidation under loose contact conditions is found to be very much appreciating within the diesel exhaust conditions.

4. Conclusions

The $LaCoO_3$, $LaFeO_3$, and $LaNiO_3$ samples prepared by citric acid sol-gel method possessed the perovskite structure, whereas the $LaZnO_y$ catalyst is a mixture of metal oxides as confirmed by XRD and FTIR. Morphological microscopy (SEM) of the explored samples demonstrated agglomerates involved mostly thin, smooth flakes and layers perforated by a large number of pores. The $LaCoO_3$ perovskite catalyst showed the highest activity for the total soot oxidation (T_{100}= 420 °C) among all the prepared catalyst samples. This can be explained due the same nano-metric range of the catalyst and soot particles. The optimum air flow rate of 150ml/min is found by experiment. Under the loose contact study, which represents the real diesel engine condition, performed on $LaCoO_3$ shows an increase of T_{100} by 52 °C as compare to tight contact, for oxidation of soot.

Acknowledgement

The authors gratefully acknowledge the financial support given to the project by the Department of Science and Technology, India under the SERC (Engineering Science) project grant DST No: SR/S3/CE/0062/2010.

References

[1] Banús, E.D., Ulla, M.A., Miró, E.E., , V.G, (2013) Structured Catalysts for Soot Combustion for Diesel Engines *http://www.intechopen.com/books/ diesel-enginecombustion-emissions-andcondition-monitoring/structured-catalysts-for-soot-combustion-for-diesel engines*, 117.

[2] Abdullah, A.Z., Abdullah, H., Bhatia, S. (2008). Improvement of Loose Contact Diesel Soot Oxidation by Synergic Effects Between Metal Oxides in K_2O-V_2O_5/ZSM-5 Catalysts. *Catalysis Communications*, 9: 1196-1200.

[3] Ramanathan, V. (2007). Global Dimming by Air Pollution and Global Warming by Greenhouse Gases: Global and Regional Perspectives. In C.D. O'Dowd and P.E. Wagner (eds). *Nucleation and Atmospheric Aerosols*: 17th International Conference Galway, Ireland, 473-483.

[4] Mishra A., Prasad, R. (2014). Preparation and Application of Perovskite Catalysts for Diesel Soot Emissions Control: An Overview. *Catalysis Review: Science and Engineering*, 56(1): 57-81.

[5] Mishra, A., Prasad, R. (2015). Development of Highly Efficient Double Substituted Perovskite Catalysts for Abatement of Diesel Soot Emissions. *Clean Technology Environmental Policy*, 17: 2337-2347.

[6] Burch, R., Coleman, M.D. (1999). An Investigation of the $NO/H_2/O_2$ Reaction on Noble-Metal Catalysts at Low Temperatures Under Lean- Burn Conditions. *Applied Catalysis: B*, 23: 115-121.

[7] Teraoka, Y., Nakano, K., Kagawa, S., Shangguan, W.F. (1995). Simultaneous Removal of Nitrogen Oxides and Diesel Soot Particulates Catalyzed by Perovskite-Type Oxides. *Applied Catalysis B: Environmental,* 5: L181-L185.

[8] Teraoka, Y., Kanada, K. Kagawa, S. (2001). Synthesis of La-K-Mn-O Perovskite Type Oxides and their Catalytic Property for Simultaneous Removal of NO*x* and Diesel Soot Particulates. *Applied Catalysis B: Environmental*, 34**:** 73-78.

[9] Russo, N., Furfori, S., Fino, D., Saracco, G., Specchia, V. (2008). Lanthanum Cobaltite Catalysts for Diesel Soot Combustion. *Applied Catalysis B: Environmental*, 83**:** 85-95.

[10] Campagnoli, E., Tavares, A., Fabbrini, L., Rossetti, I., Dubitsky, Y.A., Zaopo, A. Forni, L. (2005). Effect of Preparation Method on Activity and Stability of $LaMnO_3$ and $LaCoO_3$ Catalysts for the Flameless Combustion of Methane. *Applied Catalysis B: Environmental*, 55: 133-139.

[11] Peralta, M.A., Zanuttini, M.S., Querini, C.A. (2011). Activity and Stability of $BaKCo/CeO_2$ Catalysts for Diesel Soot Oxidation. *Applied Catalysis B: Environmental*, 110: 90-98.

[12] Nakamoto, K. (1997). *Infrared and Raman Spectra of Inorganic and Coordination Compounds, Part B, Applications in Coordination, Organometallic and Bioinorganic Chemistry*, Wiley, New York.

[13] Zhu, H.L., Yang, D.R., Yang, H., Zhu, L.M., Li, D.S., Jin, D.L., Yao, K.H. (2008). Reductive Hydrothermal Synthesis of $La(OH)_3:Tb^{3+}$ Nanorods as A New Green Emitting Phosphor. *Journal* of *Nanoparticle Research,* 10: 307-312.

[14] Zhu, L., Yu, J., Wang, X. (2007). Oxidation Treatment of Diesel Soot Particulate on $Ce_xZr_{1-x}O_2$. *Journal of Hazardous Materials*, 140: 205-210.

[15] Mu, Q., Wang, Y. (2011). Synthesis, Characterization, Shape-Preserved Transformation, and Optical Properties of $La(OH)_3$, $La_2O_2CO_3$, and La_2O_3 Nanorods. *Journal of Alloys and Compounds*, 509: 396-401.

[16] Vasudevan, S., Lakshmi, J., Sozhan, G. (2013). Electrochemically Assisted Coagulation for the Removal of Boron from Water Using Zinc Anode. *Desalination*, 310: 122-129.

[17] Guillen-hurtado, N., Lopez-Suarez, F.E., Bueno-Lopez, A., Garcia, A. (2014). Behavior of Different Soot Combustion Catalysts Under NOx/O_2. Importance of the Catalyst-Soot Contact. *Reaction Kinetics, Mechanisms, and Catalysis*, 111:167-182.